

2-Oxabicyclo[2.1.1]hexanes as saturated bioisosteres of the *ortho*-substituted phenyl ring

Received: 4 July 2022

Accepted: 25 April 2023

Published online: 5 June 2023

Check for updates

Aleksandr Denisenko¹, Pavel Garbuz¹, Nataliya M. Voloshchuk^{1,2}, Yuliia Holota³, Galeb Al-Maali^{3,4}, Petro Borysko³ & Pavel K. Mykhailiuk¹✉

The *ortho*-substituted phenyl ring is a basic structural element in chemistry. It is found in more than three hundred drugs and agrochemicals. During the past decade, scientists have tried to replace the phenyl ring in bioactive compounds with saturated bioisosteres to obtain novel patentable structures. However, most of the research in this area has been devoted to the replacement of the *para*-substituted phenyl ring. Here we have developed saturated bioisosteres of the *ortho*-substituted phenyl ring with improved physicochemical properties: 2-oxabicyclo[2.1.1]hexanes. Crystallographic analysis revealed that these structures and the *ortho*-substituted phenyl ring indeed have similar geometric properties. Replacement of the phenyl ring in marketed agrochemicals fluxapyroxad (BASF) and boscalid (BASF) with 2-oxabicyclo[2.1.1]hexanes dramatically improved their water solubility, reduced lipophilicity and most importantly retained bioactivity. This work suggests an opportunity for chemists to replace the *ortho*-substituted phenyl ring in bioactive compounds with saturated bioisosteres in medicinal chemistry and agrochemistry.

The phenyl ring is a basic structural element in chemistry. Moreover, it is one of the most common rings in bioactive compounds¹. However, organic compounds with more than two phenyl rings often have poor solubility and low metabolic stability—undesired effects in medicinal chemistry². In this context, during the last decade, the concept ‘escape from flatland’ became popular^{3,4}. Today, medicinal chemists prefer using F(*sp*³)-rich structures in drug discovery projects^{5–10}. The replacement of the phenyl ring in bioactive compounds with saturated bioisosteres has become a popular tactic to obtain novel structures with an improved physicochemical profile^{11–14}. However, most of the research in this area is devoted to the replacement of monosubstituted and *para*-disubstituted phenyl rings^{12,15–49}.

Ortho-disubstituted phenyl rings are found in more than three hundred drugs and agrochemicals (www.drugbank.ca; Fig. 1a) (ref. 50). For example, aspirin, which is widely known, contains an

ortho-disubstituted phenyl ring in its structure. In 2008, the first example of mimicking an *ortho*-disubstituted phenyl ring in a bioactive compound with a saturated bioisostere, cyclopropane, appeared in the literature (Fig. 1b) (ref. 51). Later, similar studies were performed with 1,2-disubstituted cyclopentanes and cyclohexanes (Fig. 1b) (ref. 52). In the past two years, great progress has been achieved with saturated bicyclic scaffolds, which, compared to previously used monocyclic counterparts, are intrinsically conformationally rigid. In particular, 1,2-disubstituted bicyclo[1.1.1]pentanes (Fig. 1c) (refs. 53,54) and bicyclo[2.1.1]hexanes (Fig. 1c) (refs. 55–61) were used as saturated bioisosteres of the *ortho*-disubstituted phenyl ring. In this work, we report on the preparation, characterization and biological validation of the next generation of these saturated bioisosteres, 2-oxabicyclo[2.1.1]hexanes, analogues of the *ortho*-substituted phenyl ring with improved physicochemical properties (Fig. 1c).

¹Enamine Ltd, Kyiv, Ukraine. ²National University of Life and Environmental Science of Ukraine, Kyiv, Ukraine. ³Bienta, Kyiv, Ukraine. ⁴M.G. Kholodny Institute of Botany of the National Academy of Sciences of Ukraine, Kyiv, Ukraine. ✉e-mail: Pavel.Mykhailiuk@gmail.com

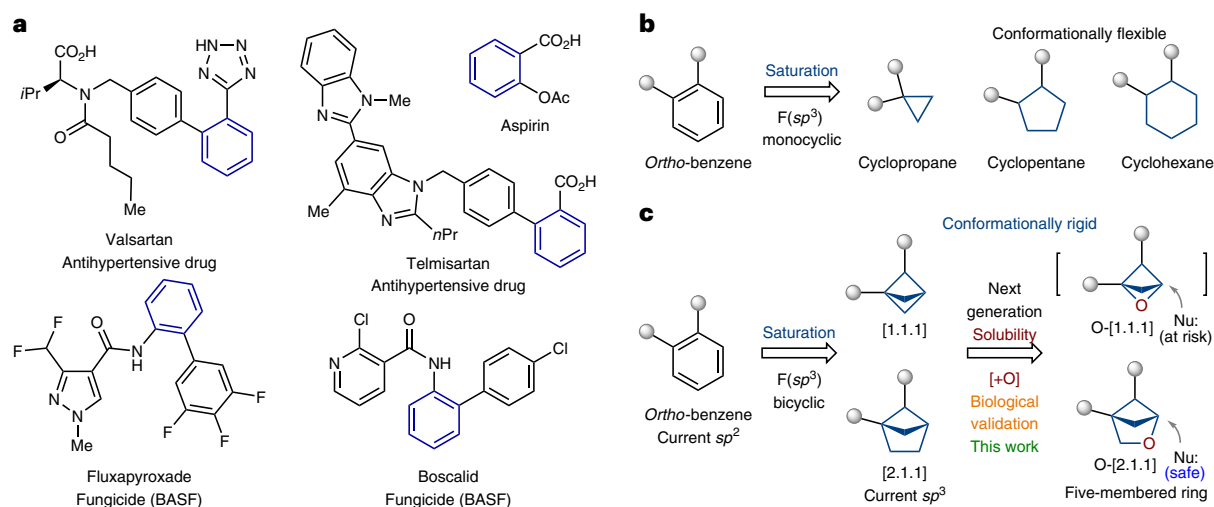


Fig. 1 | The *ortho*-substituted phenyl ring and its saturated bioisosteres. a, The *ortho*-substituted phenyl ring is a part of >300 drugs and agrochemicals. **b**, Previous examples of replacement of the *ortho*-substituted phenyl ring in bioactive compounds with monocyclic saturated rings by Qiao (2008) (ref. 51) and Shinozuka (2020) (ref. 52). **c**, Previous examples of replacement of the *ortho*-substituted phenyl ring in bioactive compounds with bicyclic saturated

scaffolds: bicyclo[1.1.1]pentane (Ma, 2020 (ref. 53); Baran, 2021 (ref. 54)) and bicyclo[2.1.1]hexane (Mykhailiuk, 2020 (ref. 55); Brown, 2022 (ref. 56); Procter, 2023 (ref. 57)). The aim of this work is the replacement of the *ortho*-substituted phenyl ring in bioactive compounds with 2-oxabicyclo[2.1.1]hexane. [+O], replacement of a methylene group ($-CH_2-$) with an oxygen atom ($-O-$).

Design

In the design of a core with a similar structure to bicyclo[1.1.1]pentanes and bicyclo[2.1.1]hexanes, but having reduced lipophilicity and enhanced water solubility, we decided to insert an oxygen atom. Replacing the methylene group in bicyclo[1.1.1]pentane with the oxygen atom leads to a strained oxetane structure (Fig. 1c), which is interesting but could be labile due to possible ring opening with nucleophiles⁶². Analogous replacement in bicyclo[2.1.1]hexanes, however, gives the substituted tetrahydrofuran (Fig. 1c). That core should be more chemically stable, so we decided to make it. From a medicinal chemistry perspective, having the ether oxygen atom in the molecule is also useful, since it could serve as an additional binding site to a receptor.

Inspiration came from our previous work, where we synthesized bridgehead disubstituted 2-oxabicyclo[2.1.1]hexanes and believed they could mimic the *meta*-disubstituted phenyl ring in bioactive compounds⁶³. This hypothesis, however, was not validated. Therefore, here we decided to prepare the disubstituted 2-oxabicyclo[2.1.1]hexanes and biologically validate them as bioisosteres of the *ortho*-disubstituted phenyl ring.

Synthesis

The photochemical [2 + 2] cycloaddition between alkenes proved to be a powerful strategy to construct cyclobutanes⁶⁴. In this context, we wondered if diene **1** (easily obtained from the commercially available starting materials; Fig. 2a) would undergo an intramolecular cyclization into the needed 2-oxabicyclo[2.1.1]hexane core. Direct irradiation of diene **1** in acetonitrile under different wavelengths gave only traces of product (Table 1, entries 1–4). Irradiation with a Hanovia broad wavelength mercury lamp gave the needed product along with many side products (entry 5). Next, we tried the addition of available organic ketones for the triplet sensitization of the styrene moiety. Indeed, smooth formation of the needed product **1a** (d.r. = 4:1) was observed under irradiation at 368 nm. The best result was obtained with benzophenone (entry 7), whereas acetophenone and substituted benzophenones also worked but provided lower yields of the end product (entries 6, 8 and 9). Among all tested solvents (entries 10–13), the best outcome was obtained in acetonitrile. Without irradiation, the reaction did not take place at room temperature or with heating (entries 14 and 15).

Under optimized conditions, cyclization of diene **1** led to a rather clean formation of a diastereomeric mixture of products **1a** (d.r. = 4:1); however, the pure major isomer **1a** was isolated by column chromatography in only 56% yield. The separation of isomers was problematic and led to a notable loss of yield, which needed to be solved.

Scaled-up synthesis

The optimized synthetic protocol is shown in Fig. 2a. It was important to identify a method that employed only available and cheap starting materials. The synthesis started from propargyl alcohol (**2**). Copper-catalysed reaction with phenyl magnesium bromide gave alcohol **3** in 71% yield following the reported procedure⁶⁵. A Michael addition of the latter with methyl propiolate (**4**) in the presence of (1,4-diazabicyclo[2.2.2]octane) (DABCO) provided the needed diene **1**. We mentioned that compound **1** partially decomposed during column chromatography and under storage at room temperature. Therefore, we decided to generate crude diene **1** in situ and use it directly in the photochemical step (Supplementary Information, page 6). A mixture of isomers **1a** was obtained. After extensive experimentation, we found a way to avoid column chromatography and not lose the yield. The crude reaction mixture after irradiation (isomers **1a** and benzophenone) was saponified with sodium hydroxide. A standard workup (removal of benzophenone) followed by crystallization from a hexane–MeOH mixture to remove the minor isomer allowed the isolation of pure major isomer **1b** at 71% yield in three steps from alcohol **3**. Product **1b** was obtained on a ten gram scale with no column purifications.

Scope

Next, we studied the scope of the developed method. The photocyclization method tolerated various substituents on the aromatic core (Table 2). Among them were alkyl groups (**5a–8a**), fluorine atoms (**9a–11a**) and chlorine atoms (**12a** and **13a**), methoxy groups (**14a–16a**) and trifluoromethyl groups (**17a–19a**). The reaction was also compatible with various substituted pyridines (**20a–24a**). In all cases, we isolated analytical quantities of intermediate esters **5a–24a** by column chromatography to characterize them. On a gram scale, however, we directly used crude reaction mixtures with **5a–24a** after photocyclization in the subsequent saponification step. In half of all cases, we could obtain the final

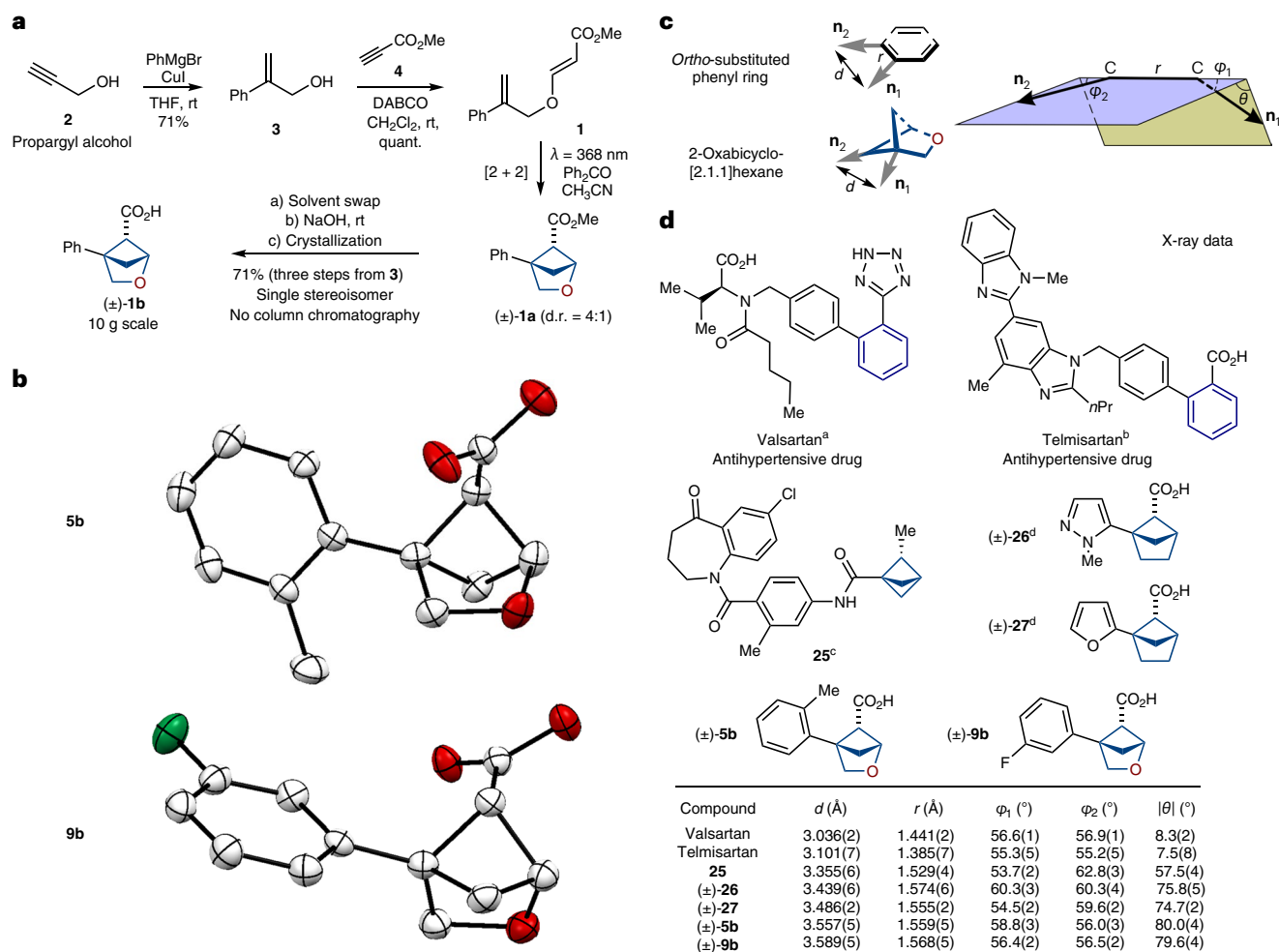


Fig. 2 | Synthesis and crystallographic analysis of 2-oxabicyclo[2.1.1]hexanes. **a**, Gram-scale synthesis of compound **1b**. THF, tetrahydrofuran; quant., quantitative. **b**, X-ray crystal structures of compounds **5b** and **9b**. Hydrogen atoms are omitted for clarity. Carbon, grey; oxygen, red; fluorine, green. **c**, Definition of vectors \mathbf{n}_1 and \mathbf{n}_2 , and geometric parameters d , r , ϕ_1 , ϕ_2 and θ . *Ortho*-

substituted phenyl ring and 2-oxabicyclo[2.1.1]hexane are shown as examples. **d**, Geometric parameters d , r , ϕ_1 , ϕ_2 and $|\theta|$ for *ortho*-substituted benzenes (valsartan, telmisartan), the saturated literature bioisosteres **25–27** and water-soluble saturated bioisosteres **5b** and **9b**. ^aData is taken from ref. 67. ^bData is taken from ref. 68. ^cData is taken from ref. 54. ^dData is taken from ref. 55.

carboxylic acids by simple crystallization of crude reaction mixtures from various solvents (Table 2). In the other half of the cases, column chromatography was still needed. The structure of carboxylic acids **5b** and **9b** was confirmed by X-ray crystallographic analysis (Fig. 2b).

Chemical stability

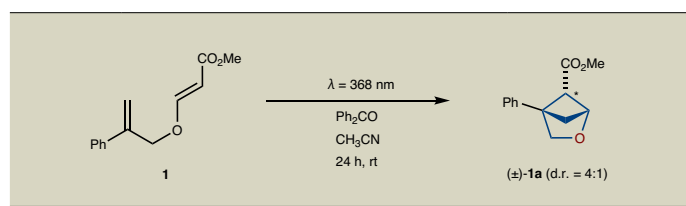
We also checked the chemical stability of three representative carboxylic acids, **1b**, **19b** and **22b** (Table 2), because we suspected that some of them could decompose via a retro-Michael-type reaction. Treatment of them with aqueous 1 M hydrochloric acid or aqueous 1 M sodium hydroxide at room temperature for one day did not lead to any decomposition. All products were crystalline solids, and we stored all of them in closed vials at room temperature on the shelf. The ¹H-NMR, liquid chromatography–mass spectrometry (LC-MS) inspection after three months did not reveal any decomposition.

Crystallographic analysis

Next, we compared the geometric parameters of 2-oxabicyclo[2.1.1]hexanes with those of the *ortho*-substituted phenyl ring and their previously suggested saturated bioisosteres, bicyclo[1.1.1]pentanes and bicyclo[2.1.1]hexanes. For that, we employed the exit vector plots tool⁶⁶. In this method, substituents at the disubstituted scaffold were

simulated by two exit vectors \mathbf{n}_1 and \mathbf{n}_2 (Fig. 2c). The relative spatial arrangement of vectors is described by four geometric parameters: the distance between C–C atoms r ; the plane angles ϕ_1 (between \mathbf{n}_1 and the C atom) and ϕ_2 (between \mathbf{n}_2 and the C atom); and the dihedral angle θ defined by vectors \mathbf{n}_1 , C–C and \mathbf{n}_2 . An additional important parameter—the distance d between two carbon substituents (Fig. 2c)—was also measured.

We calculated the values of d , r , ϕ_1 , ϕ_2 and θ of 2-oxabicyclo[2.1.1]hexanes from the X-ray data of compounds **5b** and **9b**. The related parameters for bicyclo[1.1.1]pentane **25** (ref. 54) and bicyclo[2.1.1]hexanes **26** and **27** (ref. 55) were calculated from their X-ray data published in the literature. The corresponding parameters for *ortho*-substituted phenyl rings were calculated from the reported crystal data of two antihypertensive drugs—valsartan⁶⁷ and telmisartan⁶⁸ (Fig. 2d). Analysis of this data revealed that the geometric properties of 2-oxabicyclo[2.1.1]hexanes in general were similar to those of the *ortho*-substituted phenyl ring. In particular, the distance r in 2-oxabicyclo[2.1.1]hexanes was -0.2 Å longer than that in the *ortho*-phenyl ring: 1.56–1.57 Å versus 1.38–1.44 Å, respectively. The distance d between substituents in 2-oxabicyclo[2.1.1]hexanes was also -0.5 Å longer than that in the *ortho*-phenyl ring: 3.6 Å versus 3.0–3.1 Å, respectively. Angles ϕ_1 and ϕ_2 were almost identical in both scaffolds. Moreover, ϕ_1 and

Table 1 | Optimization of the synthesis of compound 1a


Entry	Conditions	Yield (%) ^{a,b}
1	419 nm, CH ₃ CN	n.d.
2	368 nm, CH ₃ CN	<5
3	313 nm, CH ₃ CN	<5
4	254 nm, CH ₃ CN	<20
5	Hanovia mercury lamp, CH ₃ CN	39
6	368 nm, CH ₃ CN, PhC(O)Me	47
7	368 nm, CH ₃ CN, Ph ₂ CO	81 (56) ^c
8	368 nm, CH ₃ CN, (p-MeOC ₆ H ₄) ₂ CO	61
9	368 nm, CH ₃ CN, (p-NO ₂ C ₆ H ₄) ₂ CO	38
10	368 nm, CH ₂ Cl ₂ , Ph ₂ CO	71
11	368 nm, Me ₂ CO, Ph ₂ CO	68
12	368 nm, PhMe, Ph ₂ CO	42
13	368 nm, EtOAc, Ph ₂ CO	29
14	No light, rt	n.d.
15	No light, reflux	n.d.

^aReactions were performed on a 20 mmol scale. ^bThe ¹H-NMR yield of the major isomer (CH₂Br₂ as an internal standard). ^cIsolated yield of major stereoisomer of **1a**. rt, room temperature; λ, wavelength; n.d., not determined.

φ_2 in 2-oxabicyclo[2.1.1]hexanes were much closer to those in the *ortho*-phenyl ring, than to those of the previously used saturated bioisosteres: bicyclo[1.1.1]pentanes and bicyclo[2.1.1]hexanes. The difference in planarity was notable: while *ortho*-phenyl was almost flattened ($|\theta| = 7-8^\circ$), 2-oxabicyclo[2.1.1]hexanes had a substantial three-dimensional character: $|\theta| = 80^\circ$. It must be noted, however, that non-planarity was also present in bicyclo[1.1.1]pentanes ($|\theta| = 58^\circ$) and bicyclo[2.1.1]hexanes ($|\theta| = -75^\circ$; Fig. 2d).

In general, vector characteristics of 2-oxabicyclo[2.1.1]hexanes were very similar to those of the previously used bioisosteres of the *ortho*-substituted phenyl ring: bicyclo[1.1.1]pentanes and bicyclo[2.1.1]hexanes. Moreover, the important angles φ_1 and φ_2 in 2-oxabicyclo[2.1.1]hexanes were even closer to those in the *ortho*-phenyl ring than to those in bicyclo[1.1.1]pentanes and bicyclo[2.1.1]hexanes.

Incorporation into bioactive compounds

The incorporation of the 2-oxabicyclo[2.1.1]hexane scaffold into bioactive compounds was attempted next. We chose four bioactive products with the *ortho*-substituted phenyl ring: agrochemical fungicides fluxapyroxad and boscalid, antibacterial agent phthalylsulfathiazole and lipid-lowering agent lomitapide (Fig. 3).

Synthesis of the saturated analogue of fluxapyroxad was undertaken from carboxylic acid **11b** (Fig. 3a). The standard Curtius reaction followed by acylation of the intermediate amine with the substituted pyrazole carboxylic acid gave the needed compound **29**. Using an analogous tactic, compound **31**—a saturated analogue of boscalid—was also obtained from carboxylic acid **17b** (Fig. 3b). The saturated analogue of phthalylsulfathiazole was obtained by converting carboxylic acid **16b** first into the methyl ester followed by the oxidation of the phenyl ring. Amide coupling of the formed acid with the *para*-substituted aniline followed by saponification of the methyl ester gave the final

compound **33** (Fig. 3c). Amide coupling of carboxylic acid **19b** with the correspondingly *N*-substituted 4-aminopiperidine gave compound **35**, a saturated analogue of lomitapide (Fig. 3d).

In all cases, in addition to bioactive compounds with a 2-oxabicyclo[2.1.1]hexane core (**29**, **31**, **33** and **35**), we also synthesized analogous carbocyclic analogues **28**, **30**, **32** and **34** (Fig. 3 and Supplementary Information, pages 34–42).

Physicochemical parameters

In the next step, we studied the effect of the replacement of the *ortho*-phenyl ring by 2-oxabicyclo[2.1.1]hexanes on the physicochemical properties of bioactive compounds. For the comparison, we also used the corresponding carbocyclic core, bicyclo[2.1.1]hexane.

Water solubility

Replacement of the *ortho*-substituted phenyl ring in fluxapyroxad by bicyclo[2.1.1]hexane (**28**) slightly increased its solubility (Fig. 3a). However, incorporation of the 2-oxabicyclo[2.1.1]hexane in fluxapyroxad (**29**) resulted in a dramatic sixfold increase in solubility: 25 μM (fluxapyroxad) versus 34 μM (**28**) versus 155 μM (**29**). An analogous trend was also seen with boscalid and its analogues **30** and **31** (Fig. 3b). Replacement of the phenyl ring in boscalid with bicyclo[2.1.1]hexane (**30**) led to the increase of solubility by ~50%. However, the corresponding replacement with 2-oxabicyclo[2.1.1]hexane (**31**) increased the solubility by more than ten times: 11 μM (boscalid) versus 17 μM (**30**) versus 152 μM (**31**). Replacement of the phenyl ring in phthalylsulfathiazole with bicyclo[2.1.1]hexane (**32**) decreased its solubility, while the incorporation of the 2-oxabicyclo[2.1.1]hexane core (**33**) restored it: 170 μM (phthalylsulfathiazole) versus 101 μM (**32**) versus 158 μM (**33**; Fig. 3c). Lomitapide had poor solubility in water, and replacement of the phenyl ring in lomitapide with saturated bioisosteres (**34** and **35**) did not have any substantial impact on the solubility (Fig. 3d).

In summary, in two (fluxapyroxad, boscalid) out of four bioactive compounds, replacement of the *ortho*-substituted phenyl ring with 2-oxabicyclo[2.1.1]hexane led to a dramatic increase in water solubility by about one order of a magnitude.

Lipophilicity

To estimate the influence of the replacement of the *ortho*-substituted phenyl ring with saturated bioisosteres on lipophilicity, we used two parameters: calculated lipophilicity, $\log P$, where P is the partition coefficient (clogP), and experimental lipophilicity, $\log D$, where D is the distribution coefficient (logD).

Replacement of the phenyl ring with bicyclo[2.1.1]hexane either led to an increase of clogP (fluxapyroxad, boscalid; Fig. 3a,b) or did not affect it (phthalylsulfathiazole, lomitapide; Fig. 3c,d). However, in all four bioactive compounds, incorporation of 2-oxabicyclo[2.1.1]hexane instead of the *ortho*-substituted phenyl ring led to a decrease of the clogP index by about one unit.

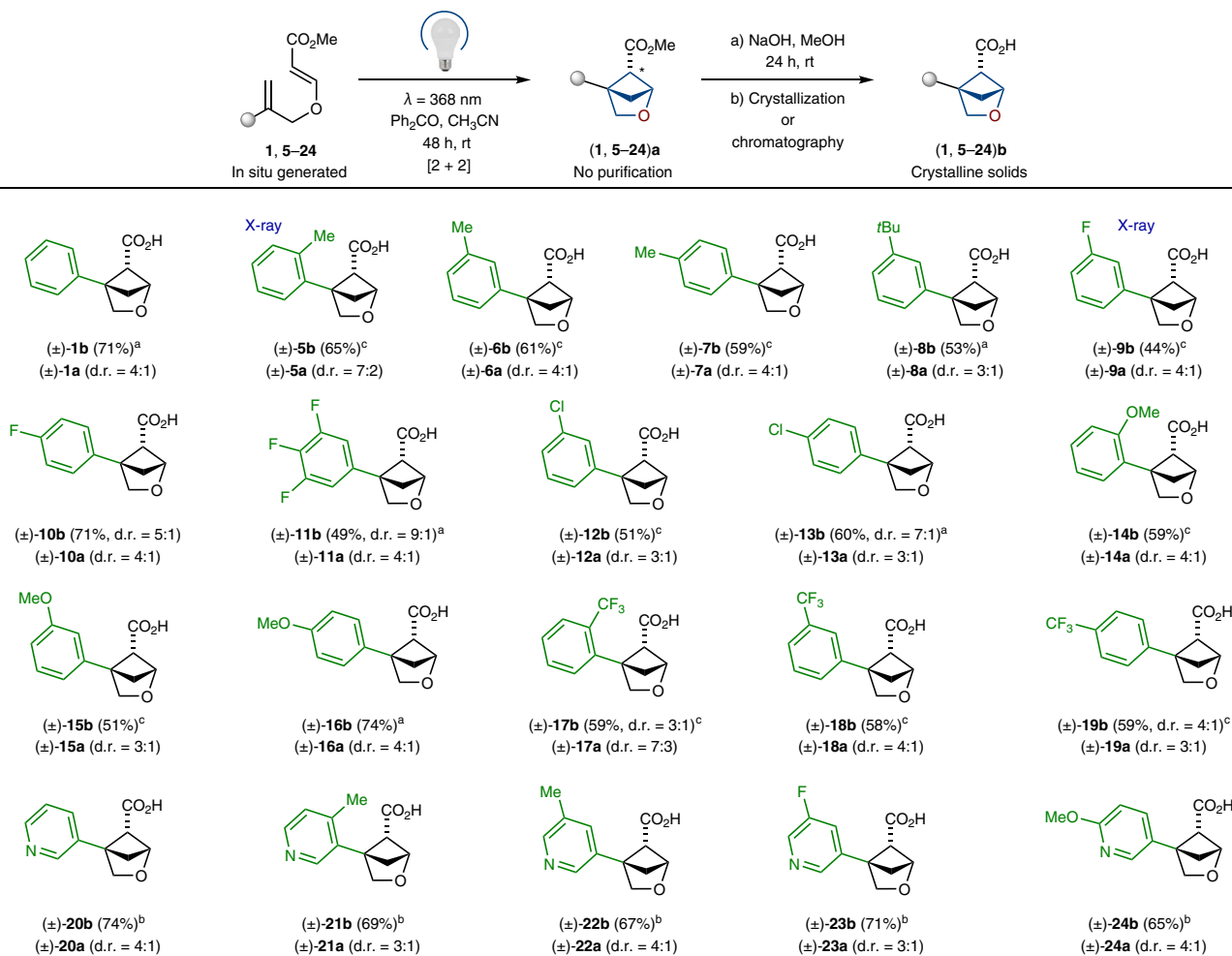
The effect of the replacement of the *ortho*-substituted phenyl ring with saturated bioisosteres on the logD index was more complex. In fluxapyroxad, incorporation of the bicyclo[2.1.1]hexane core increased logD, while the incorporation of 2-oxabicyclo[2.1.1]hexane slightly decreased it: 3.5 (fluxapyroxad) versus 4.3 (**28**) versus 2.8 (**29**; Fig. 3a). In boscalid, the incorporation of the bicyclo[2.1.1]hexane core did not affect logD substantially, while the incorporation of 2-oxabicyclo[2.1.1]hexane reduced it: 3.6 (boscalid) versus 3.5 (**28**) versus 2.7 (**29**; Fig. 3b).

In summary, in all tested compounds, replacement of the *ortho*-substituted phenyl ring with 2-oxabicyclo[2.1.1]hexane decreased the lipophilicity as measured by both clogP and logD indexes by 0.5–1.4 units.

Metabolic stability

The effect of saturated bioisosteres on the metabolic stability of bioactive compounds was complex and depended on the chemical

Table 2 | Scope of the reaction



All reactions were performed on a gram scale. Diastereomeric ratio of esters 'a' in crude reaction mixtures after the photochemical step is given. Isolated yields of acids 'b' are given in three steps from allylic alcohols. ^aProduct was isolated by crystallization from hexane–MeOtBu mixture. ^bProduct was isolated by crystallization from acetone–water mixture. ^cProduct was isolated by column chromatography.

structure. In fluxapyroxad, the incorporation of bicyclo[2.1.1]hexane (**28**) decreased the metabolic stability (Fig. 3a). However, incorporation of 2-oxabicyclo[2.1.1]hexane (**29**) unexpectedly increased it: the experimental metabolic stability in human liver microsomes, intrinsic clearance, Cl_{int} ($\text{mg min}^{-1} \mu\text{l}^{-1}$) = 28 (fluxapyroxad) versus 35 (**28**) versus 23 (**29**). In boscalid, incorporation of the bicyclo[2.1.1]hexane (**30**) increased the metabolic stability, but the incorporation of 2-oxabicyclo[2.1.1]hexane (**31**) increased it even more: Cl_{int} ($\text{mg min}^{-1} \mu\text{l}^{-1}$) = 26 (boscalid) versus 12 (**30**) versus 3 (**31**; Fig. 3b). All three compounds, phthalylsulfathiazole and its two saturated analogues **32** and **33**, were metabolically stable (Fig. 3c). In lomitapide, incorporation of the bicyclo[2.1.1]hexane core (**34**) decreased the metabolic stability, but the incorporation of the 2-oxabicyclo[2.1.1]hexane core (**35**) somewhat restored it: Cl_{int} ($\text{mg min}^{-1} \mu\text{l}^{-1}$) = 55 (lomitapide) versus 157 (**34**) versus 87 (**35**; Fig. 3d).

In summary, replacement of the *ortho*-substituted phenyl ring with 2-oxabicyclo[2.1.1]hexane in bioactive compounds improved metabolic stability (Cl_{int}) in boscalid and fluxapyroxad; slightly decreased it in lomitapide; and did not affect it in phthalylsulfathiazole.

Bioactivity

Finally, we wanted to answer a key question: can 2-oxabicyclo[2.1.1]hexanes indeed mimic the *ortho*-substituted phenyl ring in real-world

bioactive compounds? Fluxapyroxad and boscalid are marketed fungicides, developed by BASF, that have been approved for use in the United States and the European Union. Therefore, we measured their antifungal activity and compared it to that of their saturated analogues **28–31**. In strict contrast to medicinal chemistry, the use of racemic mixtures in agrochemistry is common⁵⁰; therefore for the primary validation of the proof-of-concept, we directly studied the biological activity of the available racemic compounds **28–31** (Fig. 4).

First, we measured the antifungal activity of all compounds using the agar well diffusion method (Supplementary Information, pages 238–243). Fluxapyroxad, and its saturated analogues **28** and **29**, showed a similar trend in activity at the inhibition of fungi growth (Fig. 4a,b). The 2-oxabicyclo[2.1.1]hexane analogue **29** was active, but less potent compared to the original fungicide. Compound **29** and fluxapyroxad almost identically inhibited the growth of *Fusarium oxysporum* at high concentrations; however, at low concentrations, analogue **29** showed lower activity (Fig. 4a). Similarly, **29** and fluxapyroxad effectively inhibited the growth of *Fusarium verticillioides* at high concentrations; however, at low concentrations, only fluxapyroxad remained active, while analogue **29** did not (Fig. 4b).

Boscalid and both saturated analogues **30** and **31** also effectively inhibited the fungi growth (Fig. 4c,d). However, 2-oxabicyclo[2.1.1]hexane **31** was slightly less potent than boscalid at the inhibition of

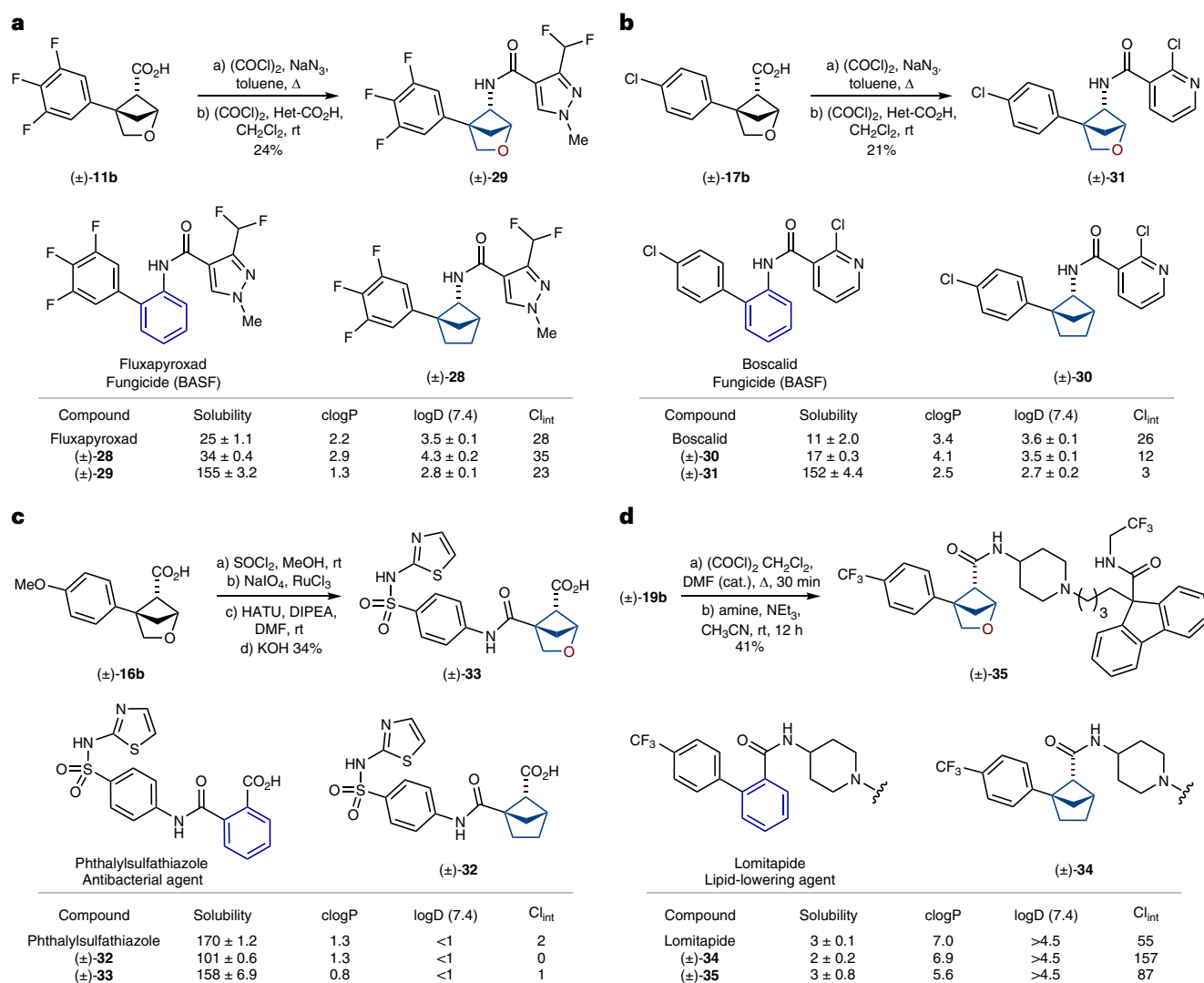


Fig. 3 | Replacement of the *ortho*-phenyl ring with saturated bioisosteres

in drugs. **a**, Synthesis and properties of compounds **28** and **29**, saturated bioisosteres of fluxapyroxad. Δ, heating; Het-CO₂H, 3-(difluoromethyl)-1-methyl-1H-pyrazole-4-carboxylic acid. **b**, Synthesis and properties of compounds **30** and **31**, saturated bioisosteres of boscalid. Het-CO₂H, 2-chloropyridine-3-carboxylic acid. **c**, Synthesis and properties of compounds **32** and **33**, saturated bioisosteres of phthalylsulfathiazole. DIPEA, *N,N*-diisopropylethylamine; DMF, dimethylformamide. **d**, Synthesis and properties of compounds **34**

and **35**, saturated bioisosteres of Lomitapide. Solubility (in μM) refers to the experimental kinetic solubility in phosphate-buffered saline at pH 7.4; clogP is the calculated lipophilicity; logD (7.4) refers to the experimental distribution coefficient in *n*-octanol/phosphate-buffered saline at pH 7.4. Reliable logD measures were obtained within a range 1.0–4.5. Cl_{int}, intrinsic clearance, experimental metabolic stability in human liver microsomes (in μl min⁻¹ mg⁻¹). cat., catalyst.

F. oxysporum (Fig. 4c) and notably less potent at the inhibition of *F. verticilloides*, especially at low concentrations (Fig. 4d).

Additionally, we measured a minimal inhibitory concentration (MIC) of all compounds (Fig. 4e). Interestingly, fluxapyroxad and its 2-oxabicyclo[2.1.1]hexane analogue **29** exhibited equal MIC values of 0.250 mg ml⁻¹ at the inhibition of the growth of *F. verticilloides*. Carbocyclic analogue **30** was two times as potent: MIC = 0.125 mg ml⁻¹. At the same time, boscalid and its 2-oxabicyclo[2.1.1]hexane analogue **31** also exhibited equal MIC values of 0.250 mg ml⁻¹ at the inhibition of the growth of *F. oxysporum*. Carbocyclic analogue **30** was much more potent: MIC = 0.031 mg ml⁻¹.

Conclusion

The *ortho*-substituted phenyl ring (as well as *meta* and *para* isomers) is a basic structural element in chemistry. In this work, we synthesized, characterized and studied 2-oxabicyclo[2.1.1]hexanes as saturated bioisosteres of the *ortho*-substituted phenyl ring (Fig. 1c). These

scaffolds were synthesized from readily available starting materials on a multigram scale. Crystallographic analysis revealed that these structures and the *ortho*-substituted phenyl ring indeed have similar geometric properties. Replacement of the *ortho*-substituted phenyl ring in bioactive compounds with 2-oxabicyclo[2.1.1]hexanes, in two out of four cases, dramatically improved water solubility (up to more than ten times) and metabolic stability. Moreover, in all four cases, such replacement also reduced lipophilicity by 0.5–1.4 clogP or logD units (Fig. 3b). In addition, the 2-oxabicyclo[2.1.1]hexanes **29** and **31** showed a similar antifungal activity compared to that of the original fungicides fluxapyroxad and boscalid.

Given the commonplace nature of the *ortho*-substituted phenyl ring in chemistry, we believe that its saturated bioisosteres described in this work will soon become very popular. One must always keep in mind, however, that the replacement of the phenyl ring in bioactive compounds with saturated isosteres can fail, if the phenyl ring is involved in integrations with the receptor: π - π stacking, π -amide

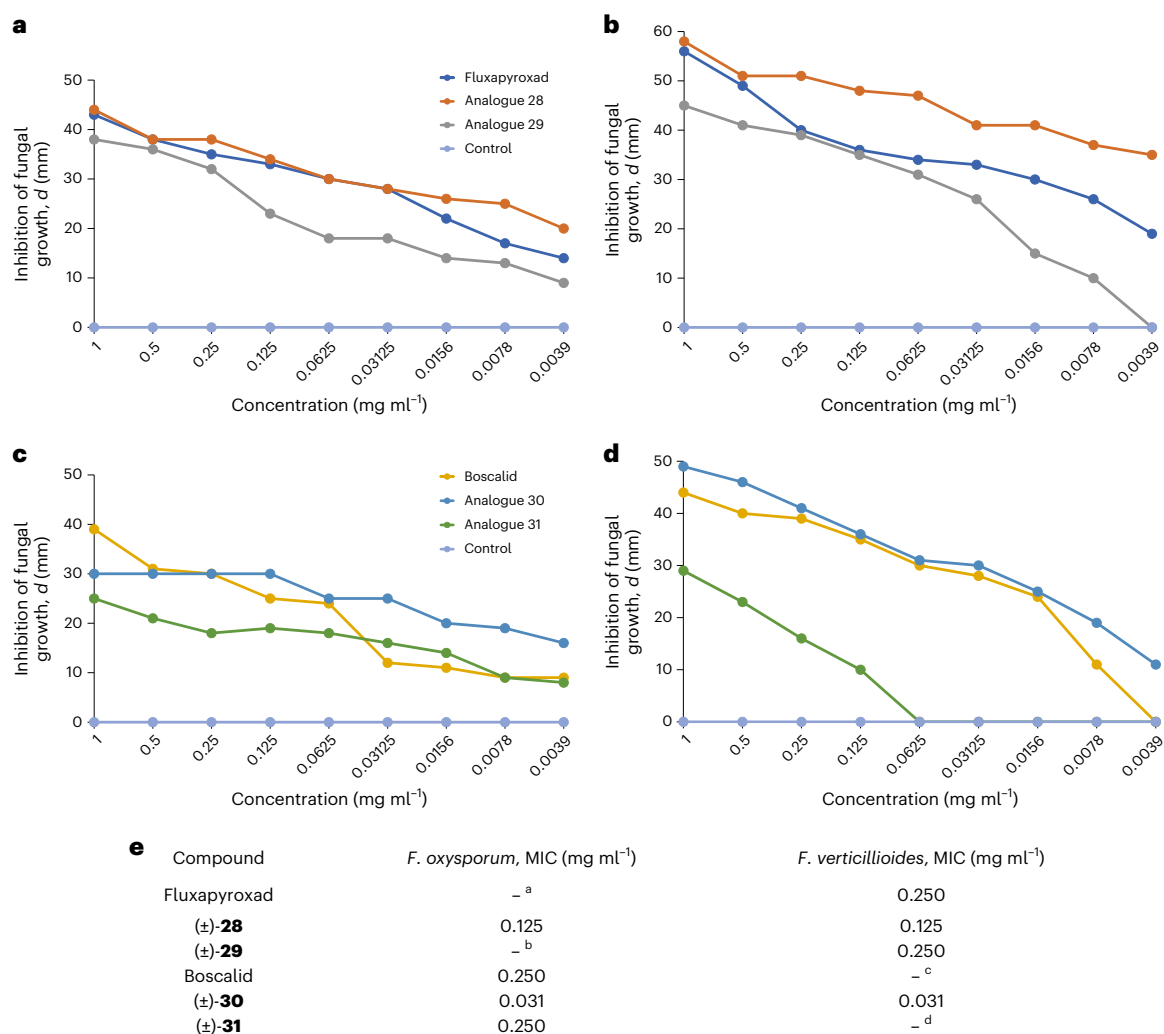


Fig. 4 | Antifungal activity of fungicides fluxapyroxad, boscalid and their saturated analogues 28–31. a, b, Inhibition of growth of *F. oxysporum* (a) and *F. verticilloides* (b; measured as a diameter *d* of the inhibition zone, in millimetres), by fluxapyroxad and its saturated analogues **28** and **29** at different concentrations after 48 h of incubation. **c, d,** Inhibition of growth of *F. oxysporum* (c) and *F. verticilloides* (d; measured as a diameter of the inhibition zone, in millimetres) by boscalid and its saturated analogues **30** and **31** at

different concentrations after 48 h of incubation. **e,** MIC for fluxapyroxad and its analogues **28** and **29**, and for boscalid and its analogues **30** and **31**. ^aMaximal inhibition of growth of *F. oxysporum* by 38.0 ± 1.9% at a concentration of 0.031 mg ml⁻¹. ^bMaximal inhibition of growth of *F. oxysporum* by 35.7 ± 2.4% at a concentration of 0.125 mg ml⁻¹. ^cMaximal inhibition of growth of *F. verticilloides* by 39.2 ± 2.7% at a concentration of 0.063 mg ml⁻¹. ^dMaximal inhibition of growth of *F. verticilloides* 36.3 ± 1.9% at a concentration of 0.250 mg ml⁻¹.

stacking, π -Asp/Glu/Arg stacking, π to amide N–H, π to O–H, π to S–H, π to ammonium salts and so on. Therefore, the replacement of the phenyl ring in bioactive compounds with saturated isosteres must be careful and balanced⁶⁹.

Online content

Any methods, additional references, Nature Portfolio reporting summaries, source data, extended data, supplementary information, acknowledgements, peer review information; details of author contributions and competing interests; and statements of data and code availability are available at <https://doi.org/10.1038/s41557-023-01222-0>.

References

- Taylor, R. D., MacCoss, M. & Lawson, A. D. G. Rings in drugs. *J. Med. Chem.* **57**, 5845–5859 (2014).
- Ritchie, T. J. & Macdonald, S. J. F. The impact of aromatic ring count on compound developability – are too many aromatic rings a liability in drug design? *Drug Discovery Today* **14**, 1011–1020 (2009).
- Lovering, F., Bikker, J. & Humblet, C. Escape from Flatland: increasing saturation as an approach to improving clinical success. *J. Med. Chem.* **52**, 6752–6756 (2009).
- Lovering, F. Escape from Flatland 2: complexity and promiscuity. *Med. Chem. Commun.* **4**, 515–519 (2013).
- Blakemore, D. C. et al. Organic synthesis provides opportunities to transform drug discovery. *Nat. Chem.* **10**, 383–394 (2018).
- Dhake, K. et al. Beyond bioisosteres: divergent synthesis of azabicyclohexanes and cyclobutenyl amines from bicyclobutanes. *Angew. Chem. Int. Ed.* **61**, e202204719 (2022).
- Stepan, A. F., Kauffman, G. W., Keefer, C. E., Verhoest, P. R. & Edwards, M. Evaluating the differences in cycloalkyl ether metabolism using the design parameter “lipophilic metabolism efficiency” (LipMetE) and a matched molecular pairs analysis. *J. Med. Chem.* **56**, 6985–6990 (2013).
- Stepan, A. F. et al. Metabolism-directed design of oxetane-containing arylsulfonamide derivatives as γ -secretase inhibitors. *J. Med. Chem.* **54**, 7772–7783 (2011).

- Yang, Y. et al. Practical and modular construction of C(sp³)-rich alkyl boron compounds. *J. Am. Chem. Soc.* **143**, 471–480 (2021).
- Simlandy, A. K., Lyu, M.-Y. & Brown, M. K. Catalytic aryloboration of spirocyclic cyclobutenes: rapid access to highly substituted spiro[3.n]alkanes. *ACS Catal.* **11**, 12815–12820 (2021).
- Stepan, A. F. et al. Application of the bicyclo[1.1.1]pentane motif as a nonclassical phenyl ring bioisostere in the design of a potent and orally active γ -secretase inhibitor. *J. Med. Chem.* **55**, 3414–3424 (2012).
- Mykhailiuk, P. K. Saturated bioisosteres of benzene: where to go next? *Org. Biomol. Chem.* **17**, 2839–2849 (2019).
- Locke, G. M., Bernhard, S. S. R. & Senge, M. O. Nonconjugated hydrocarbons as rigid-linear motifs: isosteres for material sciences and bioorganic and medicinal chemistry. *Chem. Eur. J.* **25**, 4590–4647 (2019).
- Subbaiah, M. A. M. & Meanwell, N. A. Bioisosteres of the phenyl ring: recent strategic applications in lead optimization and drug design. *J. Med. Chem.* **64**, 14046–14128 (2021).
- Gianatassio, R. et al. Strain release amination. *Science* **351**, 241–246 (2016).
- Kanazawa, J., Maeda, K. & Uchiyama, M. Radical multicomponent carboamination of [1.1.1]propellane. *J. Am. Chem. Soc.* **139**, 17791–17794 (2017).
- Makarov, I. S., Brocklehurst, C. E., Karaghiosoff, K., Koch, G. & Knochel, P. Synthesis of bicyclo[1.1.1]pentane bioisosteres of internal alkynes and *para*-disubstituted benzenes from [1.1.1]propellane. *Angew. Chem. Int. Ed.* **56**, 12774–12777 (2017).
- Lopchuk, J. M. et al. Strain-release heteroatom functionalization: development, scope, and stereospecificity. *J. Am. Chem. Soc.* **139**, 3209–3226 (2017).
- Caputo, D. F. J. et al. Synthesis and applications of highly functionalized 1-halo-3-substituted bicyclo[1.1.1]pentanes. *Chem. Sci.* **9**, 5295–5390 (2018).
- Shelp, R. A. & Walsh, P. J. Synthesis of BCP benzylamines from 2-azaallyl anions and [1.1.1]propellane. *Angew. Chem. Int. Ed.* **57**, 15857–15861 (2018).
- Hughes, J. M. E., Scarlata, D. A., Chen, A. C.-Y., Burch, J. D. & Gleason, J. L. Aminoalkylation of [1.1.1]propellane enables direct access to high-value 3-alkylbicyclo[1.1.1]pentan-1-amines. *Org. Lett.* **21**, 6800–6804 (2019).
- Wong, M. L. J., Mousseau, J. J., Mansfield, S. J. & Anderson, E. A. Synthesis of enantioenriched α -chiral bicyclo[1.1.1]pentanes. *Org. Lett.* **21**, 2408–2411 (2019).
- Nugent, J. et al. A general route to bicyclo[1.1.1]pentanes through photoredox catalysis. *ACS Catal.* **9**, 9568–9574 (2019).
- Nugent, J. et al. Synthesis of all-carbon disubstituted bicyclo[1.1.1]pentanes by iron-catalyzed Kumada cross-coupling. *Angew. Chem. Int. Ed.* **59**, 11866–11870 (2020).
- Zhang, X. et al. Copper-mediated synthesis of drug-like bicyclopentanes. *Nature* **580**, 220–226 (2020).
- Garlets, Z. J. et al. Enantioselective C–H functionalization of bicyclo[1.1.1]pentanes. *Nat. Catal.* **3**, 351–357 (2020).
- Schwärzer, K., Zipse, H., Karaghiosoff, K. & Knochel, P. Highly regioselective addition of allylic zinc halides and various zinc enolates to [1.1.1]propellane. *Angew. Chem. Int. Ed.* **59**, 20235–20241 (2020).
- Kim, J. H., Ruffoni, A., Al-Faiyz, Y. S. S., Sheikh, N. S. & Leonori, D. Divergent strain-release amino-functionalization of [1.1.1]propellane with electrophilic nitrogen-radicals. *Angew. Chem. Int. Ed.* **59**, 8225–8231 (2020).
- Yu, S., Jing, D. C., Noble, A. & Aggarwal, V. K. 1,3-Difunctionalizations of [1.1.1]propellane via 1,2-metallate rearrangements of boronate complexes. *Angew. Chem. Int. Ed.* **59**, 3917–3921 (2020).
- Yu, S., Jing, C., Noble, A. & Aggarwal, V. K. Iridium-catalyzed enantioselective synthesis of α -chiral bicyclo[1.1.1]pentanes by 1,3-difunctionalization of [1.1.1]propellane. *Org. Lett.* **22**, 5650–5655 (2020).
- Shelp, R. A. et al. Strain-release 2-azaallyl anion addition/borylation of [1.1.1]propellane: synthesis and functionalization of benzylamine bicyclo[1.1.1]pentyl boronates. *Chem. Sci.* **12**, 7066–7072 (2021).
- Wong, M. L. J., Sterling, A. J., Mousseau, J. J., Duarte, F. & Anderson, E. A. Direct catalytic asymmetric synthesis of α -chiral bicyclo[1.1.1]pentanes. *Nat. Commun.* **12**, 1644 (2021).
- Shin, S., Lee, S., Choi, W., Kim, N. & Hong, S. Visible-light-induced 1,3-aminopyridylation of [1.1.1]propellane with *N*-aminopyridinium salts. *Angew. Chem. Int. Ed.* **60**, 7873–7879 (2021).
- Pickford, H. D. et al. Twofold radical-based synthesis of *N,C*-difunctionalized bicyclo[1.1.1]pentanes. *J. Am. Chem. Soc.* **143**, 9729–9736 (2021).
- Nugent, J., Sterling, A. J., Frank, N., Mousseau, J. J. & Anderson, E. A. Synthesis of α -quaternary bicyclo[1.1.1]pentanes through synergistic organophotoredox and hydrogen atom transfer catalysis. *Org. Lett.* **23**, 8628–8633 (2021).
- Shelp, R. et al. Enantioenriched BCP benzylamine synthesis via metal hydride hydrogen atom transfer/sulfinimine addition to [1.1.1]propellane. *Org. Lett.* **24**, 110–114 (2022).
- Mousseau, J. J. et al. Automated nanomole-scale reaction screening toward benzoate bioisosteres: a photocatalyzed approach to highly elaborated bicyclo[1.1.1]pentanes. *ACS Catal.* **12**, 600–606 (2022).
- Livesley, S. et al. Electrophilic activation of [1.1.1]propellane for the synthesis of nitrogen-substituted bicyclo[1.1.1]pentanes. *Angew. Chem. Int. Ed.* **61**, e202111291 (2022).
- Polites, V. C., Badir, S. O., Keess, S., Jolit, A. & Molander, G. A. Nickel-catalyzed decarboxylative cross-coupling of bicyclo[1.1.1]pentyl radicals enabled by electron donor–acceptor complex photoactivation. *Org. Lett.* **23**, 4828–4833 (2021).
- Huang, W., Keess, S. & Molander, G. A. Dicarbofunctionalization of [1.1.1]propellane enabled by nickel/photoredox dual catalysis: one-step multicomponent strategy for the synthesis of BCP-aryl derivatives. *J. Am. Chem. Soc.* **144**, 12961–12969 (2022).
- Yen-Pon, E. et al. On-DNA hydroalkylation to introduce diverse bicyclo[1.1.1]pentanes and abundant alkyls via halogen atom transfer. *J. Am. Chem. Soc.* **144**, 12184–12191 (2022).
- Dong, W. et al. Exploiting the sp^2 character of bicyclo[1.1.1]pentyl radicals in the transition-metal-free multi-component difunctionalization of [1.1.1]propellane. *Nat. Chem.* **14**, 1068–1077 (2022).
- Mikhailiuk, P. K. et al. Conformationally rigid trifluoromethyl-substituted α -amino acid designed for peptide structure analysis by solid-state ¹⁹F NMR spectroscopy. *Angew. Chem. Int. Ed.* **45**, 5659–5661 (2006).
- Mykhailiuk, P. K., Voievoda, N. M., Afonin, S., Ulrich, A. S. & Komarov, I. V. An optimized protocol for the multigram synthesis of 3-(trifluoromethyl)bicyclo[1.1.1]pent-1-ylglycine (CF₃-Bpg). *J. Fluorine Chem.* **131**, 217–220 (2010).
- Kokhan, O. et al. Design, synthesis, and application of an optimized monofluorinated aliphatic label for peptide studies by solid-state ¹⁹F NMR spectroscopy. *Angew. Chem. Int. Ed.* **55**, 14788–14792 (2016).
- Bychek, R. & Mykhailiuk, P. K. A practical and scalable approach to fluoro-substituted bicyclo[1.1.1]pentanes. *Angew. Chem. Int. Ed.* **61**, e202205103 (2022).
- Pickford, H. D. et al. Rapid and scalable halosulfonylation of strain-release reagents. *Angew. Chem. Int. Ed.* **62**, e202213508 (2023).

48. Frank, N. et al. Synthesis of *meta*-substituted arene bioisosteres from [3.1.1]propellane. *Nature* **611**, 721–726 (2022).
49. Iida, T. et al. Practical and facile access to bicyclo[3.1.1]heptanes: potent bioisosteres of *meta*-substituted benzenes. *J. Am. Chem. Soc.* **144**, 21848–21852 (2022).
50. MacBean, C. (ed.) *The Pesticide Manual* (British Crop Production Council, 2012).
51. Qiao, J. X. et al. Achieving structural diversity using the perpendicular conformation of *alpha*-substituted phenylcyclopropanes to mimic the bioactive conformation of *ortho*-substituted biphenyl P4 moieties: discovery of novel, highly potent inhibitors of Factor Xa. *Bioorg. Med. Chem. Lett.* **18**, 4118–4123 (2008).
52. Shinozuka, T. et al. Discovery of DS-1971a, a potent, selective Na_v1.7 inhibitor. *J. Med. Chem.* **63**, 10204–10220 (2020).
53. Ma, X., Han, Y. & Bennett, D. J. Selective synthesis of 1-dialkylamino-2-alkylbicyclo-[1.1.1]pentanes. *Org. Lett.* **22**, 9133–9138 (2020).
54. Zhao, J.-X. et al. 1,2-Difunctionalized bicyclo[1.1.1]pentanes: long-sought-after mimetics for *ortho/meta*-substituted arenes. *Proc. Natl Acad. Sci. USA* **118**, e2108881118 (2020).
55. Denisenko, A., Garbuz, P., Shishkina, S. V., Voloshchuk, N. M. & Mykhailiuk, P. K. Saturated bioisosteres of *ortho*-substituted benzenes. *Angew. Chem. Int. Ed.* **59**, 20515–20521 (2020).
56. Guo, R. et al. Strain release [2 π + 2 σ] cycloadditions for the synthesis of bicyclo[2.1.1]hexanes initiated by energy transfer. *J. Am. Chem. Soc.* **144**, 7988–7994 (2022).
57. Agasti, S. et al. A catalytic alkene insertion approach to bicyclo[2.1.1]hexane bioisosteres. *Nat. Chem.* **15**, 535–541 (2023).
58. Yang, Y. et al. An intramolecular coupling approach to alkyl bioisosteres for the synthesis of multisubstituted bicycloalkyl boronates. *Nat. Chem.* **13**, 950–955 (2021).
59. Kleinmans, R. et al. Intermolecular [2 π +2 σ]-photocycloaddition enabled by triplet energy transfer. *Nature* **605**, 477–482 (2022).
60. Liang, Y., Kleinmans, R., Daniliuc, C. G. & Glorius, F. Synthesis of polysubstituted 2-oxabicyclo[2.1.1]hexanes via visible-light-induced energy transfer. *J. Am. Chem. Soc.* **144**, 20207–20213 (2022).
61. Harmata, A. S., Spiller, T. E., Sowden, M. J. & Stephenson, C. R. J. Photochemical formal (4+2)-cycloaddition of imine-substituted bicyclo[1.1.1]pentanes and alkenes. *J. Am. Chem. Soc.* **143**, 21223–21228 (2021).
62. Chalyk, B. et al. Unexpected isomerization of oxetane-carboxylic acids. *Org. Lett.* **24**, 4722–4728 (2022).
63. Levterov, V. V., Panasyuk, Y., Pivnytska, V. O. & Mykhailiuk, P. K. Water-soluble non-classical benzene mimetics. *Angew. Chem. Int. Ed.* **59**, 7161–7167 (2020).
64. Poplata, S., Tröster, A., Zou, Y.-Q. & Bach, T. Recent advances in the synthesis of cyclobutanes by olefin [2 + 2] photocycloaddition reactions. *Chem. Rev.* **116**, 9748–9815 (2016).
65. Duboudin, J. G., Jousse, B. & Saux, A. Reactifs de grignard vinyliques γ fonctionnels: I. Reactivite des organomagnesiens vis-a-vis d'alcools α acetyleniques en presence d'halogenures cuivreux. *J. Organomet. Chem.* **168**, 1–11 (1979).
66. Grygorenko, O. O., Demenko, D., Volochnyuk, D. M. & Komarov, I. V. Following Ramachandran 2: exit vector plot (EVP) analysis of disubstituted saturated rings. *New J. Chem.* **42**, 8355–8365 (2018).
67. Wang, J.-R., Wang, X., Lu, L. & Mei, X. Highly crystalline forms of valsartan with superior physicochemical stability. *Cryst. Growth Des.* **13**, 3261–3269 (2013).
68. Chadha, R., Bhandari, S., Haneef, J., Khullar, S. & Mandal, S. Cocrystals of telmisartan: characterization, structure elucidation, *in vivo* and toxicity studies. *Cryst. Eng. Comm.* **16**, 8375–8389 (2014).
69. Nicolaou, K. C. et al. Synthesis and biopharmaceutical evaluation of imatinib analogues featuring unusual structural motifs. *ChemMedChem* **11**, 31–37 (2016).

Publisher's note Springer Nature remains neutral with regard to jurisdictional claims in published maps and institutional affiliations.

Open Access This article is licensed under a Creative Commons Attribution 4.0 International License, which permits use, sharing, adaptation, distribution and reproduction in any medium or format, as long as you give appropriate credit to the original author(s) and the source, provide a link to the Creative Commons license, and indicate if changes were made. The images or other third party material in this article are included in the article's Creative Commons license, unless indicated otherwise in a credit line to the material. If material is not included in the article's Creative Commons license and your intended use is not permitted by statutory regulation or exceeds the permitted use, you will need to obtain permission directly from the copyright holder. To view a copy of this license, visit <http://creativecommons.org/licenses/by/4.0/>.

© The Author(s) 2023

Methods

General procedure for the photochemical [2 + 2] cycloaddition

The solution of diene **1** (16.79 g, 0.077 mol, 1.0 equiv.) and benzophenone (1.40 g, 0.0077 mol, 0.10 equiv.) in 850 ml of dry CH₃CN (concentration = 0.091 M) was put into a standard chemical 1 l glass flask. The reaction mixture was degassed by the bubbling of argon for 15 min. The flask was closed by a septum and irradiated with luminescent UV lamps at 368 nm (24 lamps; Sylvania 368 Blacklight F25/T8/18/BL3368; each lamp has nominal power of 25 W; total power is 600 W), under stirring at room temperature for 48 h. The reaction mixture was concentrated under reduced pressure to provide the crude product **1a** that was used in the next step (saponification) without any purification.

NMR spectra were analysed with MestreNova (11.0.3-18688).

Reporting summary

Further information on research design is available in the Nature Portfolio Reporting Summary linked to this article.

Data availability

Experimental data as well as characterization data for all new compounds prepared during these studies are provided in the Supplementary Information of this manuscript. The X-ray crystallographic coordinates for compounds **5b** and **9b** have been deposited at the Cambridge Crystallographic Data Center (CCDC) with accession codes [2166325](#) (**5b**) and [2166326](#) (**9b**). These data can be obtained free of charge from the Cambridge Crystallographic Data Center via www.ccdc.cam.ac.uk/structures/.

Acknowledgements

We are grateful to A. A. Tolmachov for the support; to I. Sadkova for the help with the preparation of the Supplementary Information; and

to S. Shishkina for the X-ray analysis of compounds **5b** and **9b**. P.K.M. is also grateful to B. Heilman for proofreading the text. This project has received funding from the European Research Council under the European Union's Horizon 2020 research and innovation programme (grant agreement no. 101000893, BENOVELTY).

Author contributions

A.D., P.G., Y.H., P.B. and P.K.M. designed the experiments. A.D., P.G., N.M.V. and G.A.-M. conducted and analysed the experiments described in this report. A.D., N.M.V., P.B. and P.K.M. prepared this manuscript for publication.

Competing interests

The authors declare the following competing interests: A.D., P.G. and P.K.M. are employees of a chemical supplier, Enamine. The remaining authors declare no competing interests.

Additional information

Supplementary information The online version contains supplementary material available at <https://doi.org/10.1038/s41557-023-01222-0>.

Correspondence and requests for materials should be addressed to Pavel K. Mykhailiuk.

Peer review information *Nature Chemistry* thanks Murugaiah Subbaiah and the other, anonymous, reviewer(s) for their contribution to the peer review of this work.

Reprints and permissions information is available at www.nature.com/reprints.

Reporting Summary

Nature Research wishes to improve the reproducibility of the work that we publish. This form provides structure for consistency and transparency in reporting. For further information on Nature Research policies, see our [Editorial Policies](#) and the [Editorial Policy Checklist](#).

Statistics

For all statistical analyses, confirm that the following items are present in the figure legend, table legend, main text, or Methods section.

- | | |
|-----|-----------|
| n/a | Confirmed |
|-----|-----------|
- The exact sample size (n) for each experimental group/condition, given as a discrete number and unit of measurement
 - A statement on whether measurements were taken from distinct samples or whether the same sample was measured repeatedly
 - The statistical test(s) used AND whether they are one- or two-sided
Only common tests should be described solely by name; describe more complex techniques in the Methods section.
 - A description of all covariates tested
 - A description of any assumptions or corrections, such as tests of normality and adjustment for multiple comparisons
 - A full description of the statistical parameters including central tendency (e.g. means) or other basic estimates (e.g. regression coefficient) AND variation (e.g. standard deviation) or associated estimates of uncertainty (e.g. confidence intervals)
 - For null hypothesis testing, the test statistic (e.g. F , t , r) with confidence intervals, effect sizes, degrees of freedom and P value noted
Give P values as exact values whenever suitable.
 - For Bayesian analysis, information on the choice of priors and Markov chain Monte Carlo settings
 - For hierarchical and complex designs, identification of the appropriate level for tests and full reporting of outcomes
 - Estimates of effect sizes (e.g. Cohen's d , Pearson's r), indicating how they were calculated

Our web collection on [statistics for biologists](#) contains articles on many of the points above.

Software and code

Policy information about [availability of computer code](#)

- | | |
|-----------------|---|
| Data collection | The irradiation experiments were performed using lamps Sylvania 368 Blacklight F25/T8/18/BL3368. Product purification was performed using HPLC AGILENT 1260 INFINITY (a column Chromatorex C18 SMB 100-5T, 100*19 mm, 5 microm) or PuriFlash XS420 Plus. The NMR data acquisition was performed using Varian UNITY III 400; Varian VNMRS 500; Bruker AVANCE DRX 500 and Bruker AVANCE III 400 spectrometers. HRMS data acquisition was performed using Agilent 6224 TOF LC/MS. Lipophilicity (clogP) was calculated with "Cxcalc" ChemAxon, version 22.5.0. |
| Data analysis | The NMR data analysis was performed using Mestrenova software (11.0.3-18688). The data acquisition and system control was performed using Analyst 1.6.3 software from AB Sciex. |

For manuscripts utilizing custom algorithms or software that are central to the research but not yet described in published literature, software must be made available to editors and reviewers. We strongly encourage code deposition in a community repository (e.g. GitHub). See the Nature Research [guidelines for submitting code & software](#) for further information.

Data

Policy information about [availability of data](#)

All manuscripts must include a [data availability statement](#). This statement should provide the following information, where applicable:

- Accession codes, unique identifiers, or web links for publicly available datasets
- A list of figures that have associated raw data
- A description of any restrictions on data availability

All data are available in the SI (Supporting Information)

Field-specific reporting

Please select the one below that is the best fit for your research. If you are not sure, read the appropriate sections before making your selection.

Life sciences Behavioural & social sciences Ecological, evolutionary & environmental sciences

For a reference copy of the document with all sections, see [nature.com/documents/nr-reporting-summary-flat.pdf](https://www.nature.com/documents/nr-reporting-summary-flat.pdf)

Life sciences study design

All studies must disclose on these points even when the disclosure is negative.

Sample size	All syntheses were performed on 100mg-20g scale. Analysis of reaction mixtures was performed with NMR and HRMS techniques. Typical sample size for analysis is 20 mg.
Data exclusions	no data were excluded from the analysis
Replication	All attempts at replication were successful. Experiments were performed minimal twice: on small scale first (20 mg), and on gram scale (5-20 g).
Randomization	not relevant in organic synthesis.
Blinding	In antifungal experiments, control tests (vehicle) were also performed.

Reporting for specific materials, systems and methods

We require information from authors about some types of materials, experimental systems and methods used in many studies. Here, indicate whether each material, system or method listed is relevant to your study. If you are not sure if a list item applies to your research, read the appropriate section before selecting a response.

Materials & experimental systems

n/a	Included in the study
<input checked="" type="checkbox"/>	<input type="checkbox"/> Antibodies
<input type="checkbox"/>	<input checked="" type="checkbox"/> Eukaryotic cell lines
<input checked="" type="checkbox"/>	<input type="checkbox"/> Palaeontology and archaeology
<input checked="" type="checkbox"/>	<input type="checkbox"/> Animals and other organisms
<input checked="" type="checkbox"/>	<input type="checkbox"/> Human research participants
<input checked="" type="checkbox"/>	<input type="checkbox"/> Clinical data
<input checked="" type="checkbox"/>	<input type="checkbox"/> Dual use research of concern

Methods

n/a	Included in the study
<input checked="" type="checkbox"/>	<input type="checkbox"/> ChIP-seq
<input checked="" type="checkbox"/>	<input type="checkbox"/> Flow cytometry
<input checked="" type="checkbox"/>	<input type="checkbox"/> MRI-based neuroimaging

Eukaryotic cell lines

Policy information about [cell lines](#)

Cell line source(s)	Single-spore isolates of <i>Fusarium oxysporum</i> Schldl. and <i>F. verticillioides</i> (Sacc.) Nirenberg (formerly known as <i>F. moniliforme</i> J. Sheld.) were obtained from organic corn plants with rot symptoms and with no previous history of exposure to any fungicides.
Authentication	Identification of <i>Fusarium</i> species was performed according to specific morphological characterization of their sporulation structure. Sing-spore isolates were grown at 20°C in complete darkness for 14 days on synthetic nutrient-poor agar (SNA) to examine the production, type, and arrangement of microconidia and conidiogenous cells. Isolates were incubated at 25°C with a 12-h photoperiod for 14 days on carnation leaf agar (CLA) to examine the shape and size of macroconidia. Microconidia, macroconidia, and chlamydoconidia were measured based on 30 random selections. Molecular genetic identification of isolates proved that they belonged to <i>Fusarium</i> genus. The verification was carried out by using method of polymerase chain reaction (PCR) with detection of amplification products in agarose gel. The DNA was extracted out by using guanidine-thiocyanate method with sorption on silicon oxide. Primers that flank part of ITS region of ribosomal DNA of <i>Fusarium</i> spp., 431 n.p. were used. After amplification in thermocycler 2720 (Applied Biosystems) with appropriate temperature mode its products were analyzed by separation in 1,5 % agarose gel. https://www.researchgate.net/publication/338875694_Interlaboratory_aprobation_of_primers_for_molecular_genetic_identification_of_Fusarium_link_fungus
Mycoplasma contamination	<i>Fusarium</i> strains were not tested for mycoplasma contamination.

Commonly misidentified lines
(See [ICLAC](#) register)

Representatives of genus *Fusarium* are ubiquitous fungi and one of the most important economic plant pathogens causing significant crop losses and contamination of grain by their secondary metabolites (mycotoxins) on a global basis. Many *Fusarium* species are causative agents of wide range of plant diseases that affect many crops including major food cultures such as wheat, barley, corn, often with social and economic impact. *Fusarium* disease is very difficult to control, because of its often development in the plant vascular system. Therefore, development of new bioactive compounds against *Fusarium* fungi is an important research in global scale.